Original article

Mechanistic study of betulinic acid extraction from *Tetracera scandens* (L.) Merr. using bio-based solvents: molecular interactions, α-glucosidase docking, and solvent cytotoxicity

Le Trong Nhan, Tran The Huan, Nguyen Thi Hoai

Faculty of Pharmacy, University of Medicine and Pharmacy, Hue University

***Corresponding author:** Nguyen Thi Hoai; email: nthoai@hueuni.edu.vn
Received: 04/02/2026; **Accepted:** 07/04/2026; **Published:** 30/04/2026
DOI: 10.34071/jmp.2026.2.951

Abstract

Background: Betulinic acid (BA) is a poorly water-soluble triterpenoid, limiting its extraction efficiency from medicinal plants and motivating the use of bio-based solvents (BioSs).

Objectives: This study aimed to elucidate the extraction mechanism of BA from *Tetracera scandens* using pentane-1,2-diol (PED) and hexane-1,2-diol (HED), to provide molecular-level insight into the potential interaction of BA with α-glucosidase using docking simulations, and to assess the cytotoxicity of the solvents.

Materials and methods: Solvent–solute interactions were investigated using quantum chemical calculations. Molecular docking simulations with α-glucosidase were performed, and the cytotoxicity of the solvents was evaluated on HEK-293A cells.

Results: PED and HED exhibited favorable interactions with BA, contributing to improved extraction efficiency. Molecular docking results indicated stable binding of BA to α-glucosidase. Both BioSs did not exhibit cytotoxic effects toward normal human cells.

Conclusion: PED and HED are promising BioSs for the extraction of BA, and the proposed solvent system demonstrates appropriate mechanistic relevance and safety for potential applications.

Keywords: *betulinic acid, Tetracera scandens, bio-based solvents, extraction mechanism, molecular docking, cytotoxicity.*

1. INTRODUCTION

Betulinic acid (BA) is a pentacyclic lupane-type triterpenoid widely distributed in numerous plant species and has attracted considerable attention due to its broad spectrum of biological activities, including anticancer, antioxidant, antidiabetic, anti-inflammatory, and antimalarial effects. Despite its pharmacological potential, the pronounced hydrophobicity and extremely low aqueous solubility of BA remain major obstacles, limiting both its extraction efficiency from plant matrices and its bioavailability in pharmaceutical and biomedical applications [1–3].

For decades, conventional organic solvents have been extensively employed for triterpenoid extraction from medicinal plants. Although these solvents often provide satisfactory extraction yields, their use is associated with several drawbacks, including toxicity, volatility, and solvent residue issues, which compromise biosafety and process sustainability. Within the framework of green chemistry and sustainable development, the identification of alternative solvents that are bio-based, environmentally benign, and safer for pharmaceutical applications has become a critical research priority [4,5].

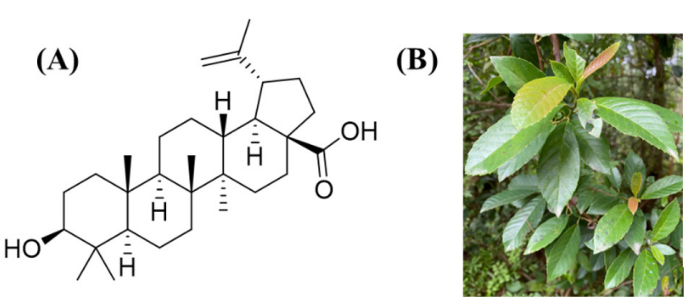

Figure 1. Chemical structures of betulinic acid (A) and *Tetracera scandens* (B)

BioSs are derived from renewable resources and are generally characterized by low toxicity and favorable biodegradability. They have been increasingly applied in pharmaceutical, food, and green chemistry fields. BioSs such as alkanediols, cyrene, gamma-valerolactone, ethyl lactate, dimethyl isosorbide, and limonene have demonstrated significant potential in enhancing the solubility and extraction efficiency of natural products. Beyond acting merely as dissolution media, many BioSs exhibit hydrotropic behavior, whereby amphiphilic solvent molecules preferentially associate around hydrophobic solutes. This mechanism reduces unfavorable solute–water interactions and markedly improves the solubility and extraction efficiency of low-polarity compounds such as triterpenoids [3,6].

Tetracera scandens (L.) Merr., belonging to the family Dilleniaceae, is a medicinal plant widely distributed in tropical regions of Asia, including Vietnam. In traditional medicine, it has been used for its antipyretic, detoxifying, anti-inflammatory, and analgesic properties, while modern studies have reported various promising biological activities. Phytochemical investigations have identified BA as one of its major constituents [3], highlighting *T. scandens* as a valuable natural source of this bioactive triterpenoid [7].

In our previous work, the extraction of BA from *T. scandens* was systematically investigated using a range of BioSs. Among them, PED and HED were identified as particularly efficient solvents, yielding higher extraction efficiencies than conventional organic solvents and several other green solvents. In addition, BA extracted using green solvents exhibited promising α-glucosidase inhibitory activity *in vitro* (IC_{50}: 7.76-7.81 μg/mL) [3]. However, the molecular extraction mechanism, deeper mechanistic insights into α-glucosidase inhibition, as well as the safety profile of these solvents have not yet been clearly elucidated.

Building on these findings and addressing the remaining knowledge gaps, the present study was designed to elucidate the extraction mechanism of BA from T. scandens using PED and HED through electrostatic potential (ESP) analysis, noncovalent interaction analysis, and binding energy calculations. In addition, preliminary mechanistic insights at the molecular level into the interaction between BA and α-glucosidase were explored using molecular docking simulations. Finally, the cellular safety of PED and HED was evaluated using HEK-293A cells to provide supporting evidence for their potential application in pharmaceutical and biomedical research.

2. MATERIALS AND METHODS

2.1. Materials and chemicals

PED and HED were purchased from Macklin Inc. (Guangzhou, China). Chemicals and reagents used for cytotoxicity assays included Dulbecco's Modified Eagle Medium (DMEM), L-glutamine, sodium pyruvate, sodium bicarbonate, fetal bovine serum (FBS), dimethyl sulfoxide (DMSO), trichloroacetic acid (TCA), Tris base, ellipticine, sulforhodamine B (SRB), acetic acid. All chemicals were of analytical grade and obtained from reputable suppliers. The HEK-293A (human embryonic kidney) cell line was supplied by National Yang Ming Chiao Tung University (Taiwan).

2.2. Quantum chemical calculations

Quantum chemical calculations were performed using the ORCA software package (version 6.1.0) [8–11](2. Initial molecular structures of BA and solvent components were constructed using Avogadro and subjected to preliminary optimization employing the MMFF94 force field [12]. Subsequent full geometry optimizations were carried out in the gas phase at the B3LYP-D3(BJ)/def2-SVP level of theory, with the RIJCOSX approximation and TightSCF convergence criteria applied to ensure computational accuracy. ESP maps, interaction region indicator (IRI) surfaces [13]in fact it also has the ability of revealing chemical bonding regions. Unfortunately, RDG cannot clearly show both types of the interactions at the same time. In this work, we propose a new real space function named interaction region indicator (IRI, and corresponding scatter plots were generated using Multiwfn (version 3.8) [14,15]. Visualization of ESP and IRI isosurfaces was conducted with VMD (version 1.9.4) [16], following standard color conventions, where blue regions indicate hydrogen bonding interactions, green regions represent van der Waals interactions, and red regions correspond to steric repulsion. The binding energy ($\mathbf{\Delta E}_{binding}$) of 1:1 solute–solvent complexes was calculated according to the equation:

$$\Delta E_{binding} = E_{complex} - (E_{solute} + E_{solvent})$$

where $E_{complex}$ is the total energy of the optimized solute–solvent complex, and E_{solute} and $E_{solvent}$ are the energies of the isolated solute and solvent molecules, respectively. Negative $\mathbf{\Delta E}_{binding}$ values indicate energetically favorable interactions between BA and the solvent.

2.3. Molecular docking simulation

Molecular docking simulations were conducted using AutoDock Vina (version 1.1.2) [17] to investigate the interaction between BA and α-glucosidase (PDB ID: 5ZCC) [18]. The enzyme structure was retrieved from the Protein Data Bank and prepared using AutoDock Tools (version 1.5.7) [19] by removing crystallographic water molecules and nonessential ligands, followed by the addition of Kollman charges and polar hydrogens. Ligand structures were drawn using ChemDraw (version 16.0), converted into three-dimensional conformations, and energy-minimized using Open Babel (version 3.1.1) [20] Chemical Markup Language. The docking protocol employed an exhaustiveness level of 64, while the binding region was defined based on the location of the co-crystallized inhibitor within the active site. Docked conformations were ranked based on binding free energy ($\Delta G_{binding}$, kcal/mol), and the most favorable binding poses were further analyzed using BIOVIA Discovery Studio (version 24.1) to elucidate hydrogen bonding and hydrophobic interactions.

2.4. Cytotoxicity assay

Cytotoxicity was evaluated using the SRB assay [21]. HEK-293A cells were cultured in DMEM supplemented with FBS, L-glutamine, and sodium bicarbonate at 37 °C in a humidified atmosphere containing 5% CO_2. Cells were seeded into 96-well plates at a density of 5,700 cells per well and treated with test samples at various concentrations. After 72 h of incubation, cells were fixed with 20% TCA and stained with 1% SRB to quantify cellular protein content. Unbound dye was removed, and protein-bound dye was solubilized with 10 mM Tris base after washing with 1% acetic acid. DMSO (10%) and ellipticine were used as negative and positive controls, respectively. Absorbance was measured at 515 nm. Cell growth inhibition (I%) was calculated using the following equation:

$$I\% = (1 - (OD_t - OD_0)/(OD_c - OD_0)) \times 100\%$$

where OD_0, OD_t, OD_c correspond to the optical density at the initial time point, after 72 h of treatment, and of the control, respectively.

3. RESULTS

3.1. Extraction mechanism

3.1.1. ESP analysis and binding energy evaluation

ESP analysis is a widely used quantum chemical tool that provides insight into the surface charge distribution of molecules, thereby allowing the identification of electron-rich and electron-deficient regions that are prone to intermolecular interactions [22]. In this study, ESP analysis was employed to elucidate the charge distribution on the molecular surface of BA and to identify regions potentially involved in solvent interactions. The ESP map of BA revealed a pronounced amphiphilic character (**Figure 2A**). Negative electrostatic potential was mainly localized around the carboxyl group and oxygen atoms, indicating their strong propensity for hydrogen bonding and dipole–dipole interactions. In contrast, the triterpenoid backbone exhibited predominantly low-polarity characteristics, suggesting the necessity of a solvent environment capable of stabilizing both polar and nonpolar domains of the molecule.

To quantitatively assess solvent–solute interactions, binding energies between BA and different solvents were calculated and are summarized in **Figure 2B**. The BA–H_2O, BA-MeOH, BA-EtOH systems exhibited relatively low binding energies, with values of -11.960, -12.909, and -12.545 kcal/mol, respectively. These results indicate that interactions in these systems are mainly governed by localized hydrogen bonding at polar functional groups, while the extensive hydrophobic triterpenoid framework remains insufficiently stabilized. Consequently, within the simplified 1:1 interaction model, conventional polar solvents show limited capability to provide spatially extensive interaction coverage across the BA molecular surface.

In contrast, substantially more negative binding energies were obtained for the betulinic acid–pentan-1,2-diol (BA-PED) and betulinic acid–hexan-1,2-diol (BA-HED) systems, reaching -22.902 and -23.843 kcal/mol, respectively. These markedly enhanced interactions reflect a cooperative solvation mechanism, in which the hydroxyl groups of the alkanediols engage in directional hydrogen bonding with the polar regions of BA, while the hydrocarbon chains contribute to stabilizing the hydrophobic backbone through van der Waals and hydrophobic interactions. This dual interaction mode enables BA to be accommodated within a more favorable solvation microenvironment, rather than being stabilized only at isolated polar sites.

Although all investigated systems contained water, the binding energy analysis clearly demonstrates that PED and HED play a dominant role in governing BA–solvent interactions. The significantly stronger interactions between BA and the BioSs compared with BA–H_2O interactions indicate that water alone cannot account for the observed solubilization and

stabilization. Instead, the BioSs generate a tailored electrostatic and hydrophobic microenvironment capable of simultaneously stabilizing both polar and nonpolar regions of BA, thereby providing a mechanistic explanation for the enhanced extraction efficiency observed experimentally [3].

It should be noted that PED and HED are conformationally flexible molecules with multiple possible rotamers, and the optimized structures obtained in this study correspond to energetically favorable local minima. Although global minimum conformations were not exhaustively explored, the use of a consistent computational protocol across all systems ensures reliable comparative analysis of solvent–solute interactions. Moreover, the key interaction sites of PED and HED (e.g., hydroxyl groups and alkyl chains) are preserved across low-energy conformers, suggesting that the primary interaction patterns are not expected to change significantly. In addition, the 1:1 solute–solvent interaction model represents a simplified approach to capture the primary interaction motif between BA and solvent molecules and has been widely employed in previous studies to evaluate intermolecular interactions [23,24]a biphasic temperature-responsive solvent system consisting of hydrophilic deep eutectic solvent (choline chloride: levulinic acid. While real systems involve multiple solvent molecules and dynamic interactions, this model provides a fundamental and comparable framework for evaluating relative interaction strengths across different solvent systems, particularly for mechanistic interpretation.

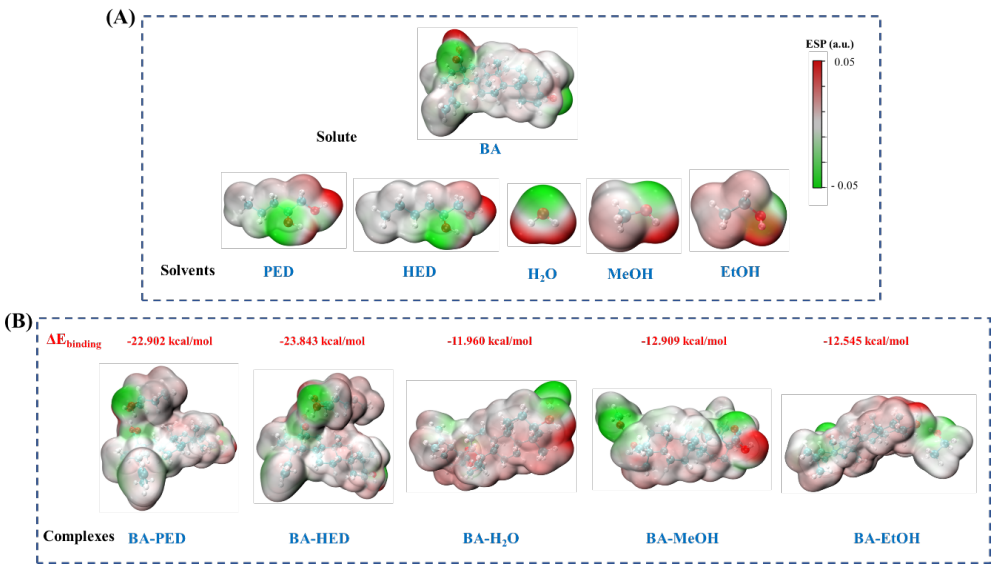

Figure 2. ESP maps of BA and the investigated solvents, together with the interaction geometries and binding energies of the BA–PED, BA–HED, BA–H_2O, BA–MeOH, and BA–EtOH systems.

3.1.2. IRI analysis of noncovalent interactions

To obtain deeper mechanistic insight into BA–solvent interactions, IRI analysis was conducted in conjunction with IRI scatter plots derived from sign(λ_2)ρ values and the corresponding isosurfaces. This approach allows clear differentiation between weak attractive interactions, such as hydrogen bonding and van der Waals forces, as well as steric repulsive regions.

For the BA–H_2O system (**Figure 3C**), the IRI scatter plot displayed data points primarily located in the slightly negative sign(λ_2)ρ region, characteristic of weak attractive interactions. The corresponding IRI isosurfaces were mainly localized around the carboxyl group and oxygen atoms of BA, indicating the formation of limited hydrogen bonds with water molecules. However, these interactions were spatially confined and did not substantially extend over the hydrophobic triterpenoid backbone, suggesting limited overall molecular stabilization.

A similar interaction pattern was observed for the BA–MeOH and BA–EtOH systems (**Figures 3D** and **3E**). Although the number of interaction regions slightly increased compared with water, the IRI isosurfaces remained concentrated near the polar functional groups of BA and did not substantially extend along the carbon framework. This finding indicates that conventional polar solvents offer only modest improvements in BA–solvent interactions and are insufficient to establish a comprehensive

stabilization environment.

In contrast, the BA–PED and BA–HED systems exhibited distinctly different interaction profiles in both IRI scatter plots and isosurface visualizations (**Figures 3A** and **3B**). In addition to pronounced hydrogen bonding between the hydroxyl groups of the alkanediols and the carboxyl group of BA, an extensive and continuous network of van der Waals interactions was observed along the triterpenoid skeleton. These regions, characterized by sign(λ_2)ρ values close to zero, correspond to weak but spatially extensive attractive interactions that play a critical role in stabilizing the hydrophobic domains of BA.

Overall, IRI analysis demonstrates that aqueous solutions of PED and HED generate a more diverse and spatially distributed noncovalent interaction network around BA compared with water and conventional polar solvents. The synergistic combination of localized hydrogen bonding and extended van der Waals interactions contributes to the formation of a favorable solvation microenvironment, reinforcing the central role of BioSs in the BA extraction mechanism observed experimentally [3].

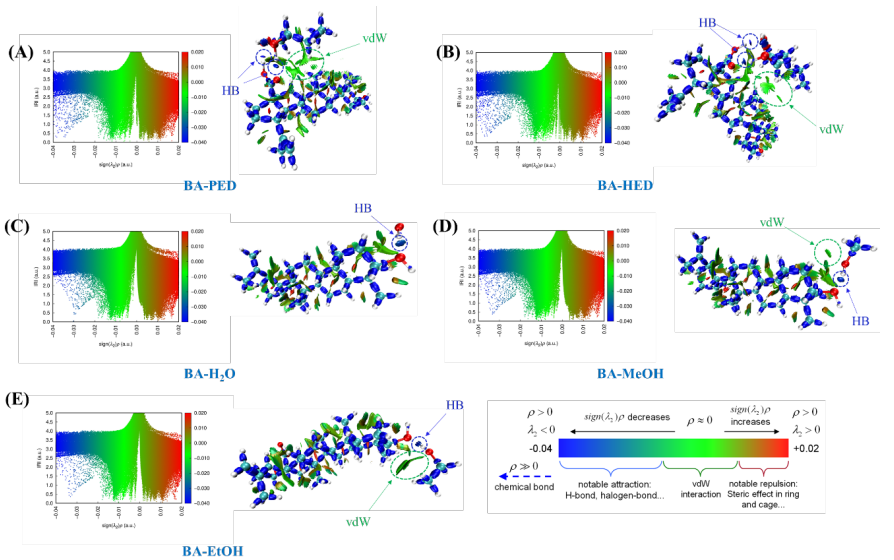

Figure 3. IRI scatter plots as a function of sign(λ_2)ρ and corresponding IRI isosurfaces illustrating noncovalent interactions between betulinic acid (BA) and PED, HED, H_2O, MeOH, and EtOH. HB denotes hydrogen bonding interactions and vdW denotes van der Waals interactions.

3.4. Molecular docking analysis for α-glucosidase inhibition

Previous studies have reported that BA-rich extracts obtained using green solvents exhibit notable α-glucosidase inhibitory activity [3], suggesting that BA may contribute substantially to this effect. To gain mechanistic insight at the molecular level, *in silico* molecular docking was performed to evaluate the binding affinity and interaction pattern between BA and α-glucosidase, with acarbose used as a reference inhibitor.

Docking results revealed that BA binds stably within the active site of α-glucosidase, with a binding energy of −8.1 kcal/mol, which is comparable to that of the reference inhibitor acarbose (−7.7 kcal/mol) within the limitations of docking-based scoring functions. The more negative binding energy of BA suggests a favorable binding propensity and a stable binding mode within the docking model.

Analysis of the binding conformation showed that BA is appropriately positioned within the catalytic pocket of α-glucosidase (**Figure 4**). The hydrophobic triterpenoid framework of BA is primarily stabilized through an extensive network of van der Waals interactions with hydrophobic amino acid residues located within the active site. Meanwhile, oxygen-containing functional groups of BA serve as anchoring points for directional hydrogen bonding interactions with neighboring residues, contributing to the stabilization and orientation of the ligand.

Collectively, these *in silico* results provide molecular-level evidence supporting the favorable and stable interaction between BA and α-glucosidase, thereby offering mechanistic support for the α-glucosidase inhibitory activity observed in previous experimental studies.

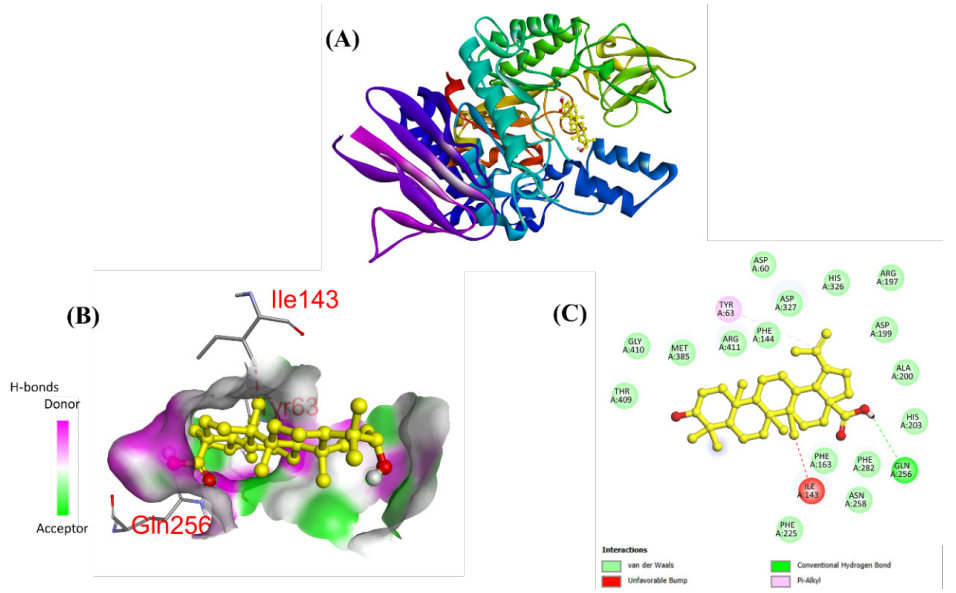

Figure 4. Molecular docking results of BA with α-glucosidase (PDB: 5ZCC): (A) overall structure of the enzyme–ligand complex; (B) binding position of BA within the active site; (C) noncovalent interactions between BA and amino acid residues.

3.5. Cytotoxicity evaluation of PED and HED

To assess the biocompatibility of the BioSs employed, the cytotoxicity of PED and HED toward HEK-293A cells was systematically investigated, thereby confirming that improved extraction efficiency did not compromise normal cell viability. This cell line is commonly employed as a representative non-cancerous model for in vitro toxicity screening.

As summarized in Table 1, PED and HED showed no appreciable reduction in HEK-293A cell viability, with IC_{50} values above 100 µg/mL. This cytotoxicity profile supports their favorable biocompatibility across the investigated concentration range. Importantly, this result supports the safe application of these BioSs in biological studies and further underscores their suitability for sustainable and biomedically relevant extraction processes.

Table 1. Cytotoxicity of PED and HED in HEK-293A cells.

Solvents/compound	IC_{50} values (µg/mL)
PED	> 100
HED	> 100
Ellipticine	0.30 ± 0.02

4. DISCUSSION

This study provides a comprehensive approach to elucidating the relationship between extraction efficiency, molecular interaction mechanisms, and the mechanistic relevance of BA obtained from *T. scandens* using BioSs. Analyses based on ESP, binding energy calculations, and IRI consistently demonstrate that BA is a distinctly amphiphilic molecule, characterized by an uneven distribution between a highly polar carboxyl moiety and a predominantly nonpolar triterpenoid framework. This structural feature explains why conventional polar solvents such as water, methanol, and ethanol predominantly engage in localized interactions through hydrogen bonding at polar functional groups, while less effective in stabilizing the hydrophobic backbone of the molecule. As a result, relatively low binding energies are observed, leading to limited solubilization capacity and restricted extraction efficiency of BA.

In contrast, alkanediol-based BioSs, exemplified by PED and HED, exhibit a characteristic cooperative interaction mechanism. The hydroxyl groups of these solvents participate in directional hydrogen bonding with the carboxyl group of BA, while the longer hydrocarbon chains facilitate the formation of an extended network of van der Waals interactions with the triterpenoid skeleton. This synergistic combination generates a favorable solvation microenvironment that stabilizes the entire BA molecule rather than only isolated polar regions. This behavior is clearly reflected by the substantially more negative binding energies of BA–alkanediol systems compared with conventional solvents and

is consistent with the enhanced extraction efficiency observed experimentally.

Molecular docking simulations, on the other hand, provided supportive *in silico* evidence for a plausible binding interaction of BA with the α-glucosidase enzyme. Detailed docking analysis revealed that BA is favorably accommodated within the active site of α-glucosidase through a diverse network of noncovalent interactions involving key amino acid residues. Specifically, the carboxyl group of BA forms a hydrogen bond with the Gln256 residue, serving as a directional anchoring point that contributes to stabilization of the binding pose. In addition, the hydrophobic triterpenoid framework of BA interacts extensively with surrounding residues such as Thr409, Gly410, Met385, Arg441, Phe144, Asp327, Asp60, His326, Arg197, Asp199, Ala200, His203, Phe163, Phe282, Phe225, and Asn258 through van der Waals interactions. These interactions create an extensive molecular contact surface, allowing BA to adapt effectively to the hydrophobic environment of the α-glucosidase active pocket. Notably, the presence of a π-alkyl interaction with Tyr63 highlights the role of aromatic residues in stabilizing the polycyclic carbon scaffold of BA. Although these interactions are less directional than hydrogen bonds, they contribute to the formation of a surrounding interaction environment that evenly distributes binding forces and contributes to the overall favorability of the binding interaction. A localized unfavorable interaction with Ile143 was also observed; however, this interaction does not appear to significantly compromise the predicted binding mode, as it is compensated by the surrounding hydrophobic and hydrogen bonding interactions. Such localized unfavorable contacts are commonly encountered in docking models of bulky hydrophobic compounds and do not significantly affect the overall binding affinity of the ligand. Collectively, the docking results suggest that BA may interact with α-glucosidase through a combination of directional hydrogen bonding and hydrophobic interactions, which may help rationalize the α-glucosidase inhibitory activity reported in previous experimental studies.

Finally, cytotoxicity evaluation demonstrated that PED and HED do not exert significant adverse effects on HEK-293A cells within the investigated concentration range. This finding is of particular importance, as it confirms that the enhancement in extraction efficiency and molecular interaction capability is not accompanied by increased cellular toxicity. Consequently, these results support the suitability of PED and HED as biocompatible BioSs for biomedical research and the development of sustainable extraction processes.

5. CONCLUSION

This study elucidated the extraction mechanism of BA from *T. scandens* using BioSs. Quantum chemical analyses revealed favorable solvent–solute interactions, providing a molecular rationale for the enhanced extraction efficiency of BA achieved with PED and HED. Molecular docking simulations further provided preliminary *in silico* insight into the binding behavior of BA within the α-glucosidase active site, which may help rationalize its reported enzyme inhibitory activity. In addition, PED and HED did not exhibit cytotoxic effects toward normal human cells within the tested concentration range. Overall, these findings support the suitability of PED and HED as effective and biocompatible BioSs for the green extraction of BA from medicinal plants.

Acknowledgements

This work was supported by Hue University under the Core Research Program, Grant No. NCTB. DHH.2026.07. Nhan Trong Le was funded by the PhD Scholarship Programme of Vingroup Innovation Foundation (VINIF), VinUniversity, code VINIF.2025. TS58.

REFERENCES

1. Fernandes S, Vieira M, Prudêncio C, Ferraz R. Betulinic Acid for Glioblastoma Treatment: Reality, Challenges and Perspectives. Int J Mol Sci 2024;25:2108.

2. Aswathy M, Vijayan A, Daimary UD, Girisa S, Radhakrishnan K V, Kunnumakkara AB. Betulinic acid: A natural promising anticancer drug, current situation, and future perspectives. J Biochem Mol Toxicol 2022;36:e23206.

3. Le NT, Nguyen LT, Thi Nguyen NA, Nguyen HT. Unlocking the potential of bio-based solvents for sustainable triterpenoid extraction: a case study on betulinic acid from *Tetracera scandens* (L.) Merr. Sep Purif Technol 2025;370:133196.

4. Yannick PD, Gijsbert Tjalsma T, Su Z, Malankowska M, Pinelo M. What is next? the greener future of solid liquid extraction of biobased compounds: Novel techniques and solvents overpower traditional ones. Sep Purif Technol 2023;320:124147.

5. Huang MM, Yiin CL, Mun Lock SS, Fui Chin BL, Othman I, binti Ahmad Zauzi NS, et al. Natural deep eutectic solvents (NADES) for sustainable extraction of bioactive compounds from medicinal plants: Recent advances, challenges, and future directions. J Mol Liq 2025;425:127202.

6. Silva SS, Justi M, Chagnoleau J-B, Papaiconomou N, Fernandez X, Santos SAO, et al. Using biobased solvents

for the extraction of phenolic compounds from kiwifruit industry waste. Sep Purif Technol 2023;304:122344.

7. Nokhala A, Siddiqui MJ. Phytochemicals and biological activity of *Tetracera scandens* Linn. Merr. (Dilleniaceae): A short review. J Pharm Bioallied Sci 2020;12:217–22.

8. Neese F. Software Update: The ORCA Program System—Version 6.0. WIREs Comput Mol Sci 2025;15:e70019.

9. Neese F. An improvement of the resolution of the identity approximation for the formation of the Coulomb matrix. J Comput Chem 2003;24:1740–7.

10. Garcia-Ratés M, Neese F. Effect of the Solute Cavity on the Solvation Energy and its Derivatives within the Framework of the Gaussian Charge Scheme. J Comput Chem 2020;41:922–39.

11. Neese F. The SHARK integral generation and digestion system. J Comput Chem 2023;44:381–96.

12. Hanwell MD, Curtis DE, Lonie DC, Vandermeersch T, Zurek E, Hutchison GR. Avogadro: an advanced semantic chemical editor, visualization, and analysis platform. J Cheminform 2012;4:17.

13. Lu T, Chen Q. Interaction Region Indicator: A Simple Real Space Function Clearly Revealing Both Chemical Bonds and Weak Interactions. Chemistry–Methods 2021;1:231–9.

14. Lu T, Chen F. Multiwfn: A multifunctional wavefunction analyzer. J Comput Chem 2012;33:580–92.

15. Lu T. A comprehensive electron wavefunction analysis toolbox for chemists, Multiwfn. J Chem Phys 2024;161:82503.

16. Humphrey W, Dalke A, Schulten K. VMD: Visual molecular dynamics. J Mol Graph 1996;14:33–8.

17. Trott O, Olson AJ. AutoDock Vina: Improving the speed and accuracy of docking with a new scoring function, efficient optimization, and multithreading. J Comput Chem 2010;31:455–61.

18. Auiewiriyanukul W, Saburi W, Kato K, Yao M, Mori H. Function and structure of GH13_31 α-glucosidase with high α-(1→4)-glucosidic linkage specificity and transglucosylation activity. FEBS Lett 2018;592:2268–81.

19. Morris GM, Huey R, Lindstrom W, Sanner MF, Belew RK, Goodsell DS, et al. AutoDock4 and AutoDockTools4: Automated docking with selective receptor flexibility. J Comput Chem 2009;30:2785–91.

20. O'Boyle NM, Banck M, James CA, Morley C, Vandermeersch T, Hutchison GR. Open Babel: An open chemical toolbox. J Cheminform 2011;3:33.

21. Skehan P, Storeng R, Scudiero D, Monks A, McMahon J, Vistica D;., et al. New Colorimetric Cytotoxicity Assay for Anticancer-Drug Screening. J Natl Cancer Inst 1990;82:1107–12.

22. Wang N, Tian Y, Wu X, Liu H, Lu H, Zhu Y. Natural Hydrophobic Deep Eutectic Solvent for Highly Efficient Extraction of Curcuminoids Assisted by Pulsed Ultrasound: Experimental and Mechanistic Insights. ACS Sustain Chem Eng 2025;13:9087–97.

23. Cai Z-H, Dong X-Y, Wang L-T, Zhou W-M, Wang Y-N, Yang J, et al. A novel temperature-responsive biphasic deep eutectic solvent-based solvent system: Integrated efficient extraction, enrichment and recovery of phytochemicals. Chem Eng J 2024;499:156012.

24. Cai Z-H, Wang J-D, Liu L, Ruan L-D, Gu Q, Yan X-Y, et al. A green and designable natural deep eutectic solvent-based supramolecular solvents system: Efficient extraction and enrichment for phytochemicals. Chem Eng J 2023;457:141333.